Nanosecond Photothermal Effects in Plasmonic Nanostructures

Xi Chen,[†] Yiting Chen,[†] Min Yan,[†] and Min Qiu[†,‡,*]

[†]Laboratory of Photonics and Microwave Engineering, School of Information and Communication Technology, KTH Royal Institute of Technology, Electrum 229, 16440 Kista, Sweden, and [‡]State Key Laboratory of Modern Optical Instrumentation, Department of Optical Engineering, Zhejiang University, 310027, Hangzhou, China

ABSTRACT

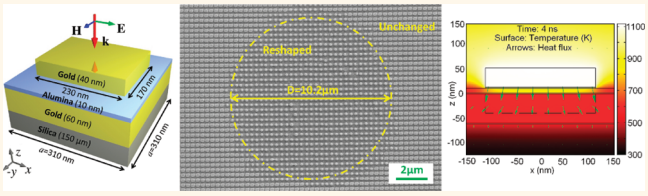

Photothermal effects in plasmonic nanostructures have great potentials in applications for photothermal cancer therapy, optical storage, thermo-photovoltaics, *etc.* However, the transient temperature behavior of a nanoscale material system during an ultrafast photothermal process has rarely been accurately investigated. Here a heat transfer model is constructed to investigate the temporal and spatial variation of temperature in plasmonic gold nanostructures. First, as a benchmark scenario, we study the light-induced heating of a gold nanosphere in water and calculate the relaxation time of the nanosphere excited by a modulated light. Second, we investigate heating and reshaping of gold nanoparticles in a more complex metamaterial absorber structure induced by a nanosecond pulsed light. The model shows that the temperature of the gold nanoparticles can be raised from room temperature to >795 K in just a few nanoseconds with a low light luminance, owing to enhanced light absorption through strong plasmonic resonance. Such quantitative predication of temperature change, which is otherwise formidable to measure experimentally, can serve as an excellent guideline for designing devices for ultrafast photothermal applications.

KEYWORDS: thermodynamic · photothermal · metamaterial absorber · nanoparticle reshaping

Metal nanoparticles (NPs) show strong scattering and absorption of light in visible and near-infrared region owing to their localized plasmon resonances. The absorbed light is then turned into thermal energy. With pulsed light irradiation, transient thermal power generated in NPs introduces abundant thermodynamic effects, such as ablation, ultrafast heating, thermal expansion, surface melting, and reshaping. The heat transfer theory of ultrafast laser heating was explored in the last century by Kaganov *et al.*,[1] Anisimov *et al.*,[2] Qiu *et al.*,[3] and others. Much experimental work has also been done recently, due to rapid developments in nanotechnology. For example, Link and coworkers[4] showed that various degrees of shape change of gold nanorods in a colloid can be induced by using an intense femtosecond- and nanosecond-pulsed laser; Hu and Hartland[5] investigated the relaxation time of heat dissipation for gold NPs in aqueous solution with femtosecond-pulsed laser heating; Plech and co-workers[6,7] used time-resolved X-ray scattering to examine the lattice dynamics of gold NPs excited by a femtosecond laser, and found that gold NPs enter the premelt state when lattice temperature is only 519 K; Govorov and coworkers[8] showed that laser-heated gold NPs leads to the melting of ice matrix; Baffou and co-workers presented a thermal microscopy method based on molecular fluorescence and imaged the heat source distribution of the NPs system.[9] The laser-heated NP system already showed potential applications in NP fabrication,[10,11] photothermal therapy,[12] drag delivery,[13] and optical data storage.[14]

However, to the best of the authors' knowledge, the transient temperature variation of a nanoscale material system during an ultrafast photothermal process has rarely been accurately characterized. Only indirect measurements have so far been attempted.[5−7] Lack of quantitative assessment of photothermal effect in a plasmonic system can greatly obstruct device design and optimization. Numerical calculation of photothermal response, on the other hand, can quickly reveal temperature information in a complex plasmonic nanostructure, which has indeed attracted some attention recently. Baffou and co-workers[15] presented a boundary element method for solving electromagnetic scattering and steady-state heat transfer analysis of gold NPs in water excited by a continuous-wave (CW) laser. In another work, Baffou and Rigneault[16] introduced a numerical approach

* Address correspondence to min@kth.se.

Received for review December 20, 2011 and accepted February 22, 2012.

Published online February 22, 2012
10.1021/nn2050032

based on the finite difference method to investigate the transient temperature of gold NPs in water excited by femtosecond-pulsed laser. In this paper, we build a heat transfer model to quantitatively understand the light-induced heating in nanoscaled plasmonic systems. Both the electromagnetic-absorption and the heat-transfer portions of the multiphysics model are solved with the versatile and commercially available finite element method (FEM). To keep the validity of heat transfer equation in our system, we have to take care of the spatial and temporal extremities: first, we take account of the correction of the material properties such as thermal conductivity,[17] boundary thermal conductance,[18−20] and melting point,[21] due to nanometer size effect, Second, we restrict the application of the heat transfer equation only to problems with a light pulse duration of nanoseconds or longer, because a femtosecond or picosecond laser pulse introduces nonequilibrium between electrons and the lattice of a material. Two study cases will be presented in our model. First, we will discuss the case of exciting a gold nanosphere in water by CW laser and the thermal relaxation time of such a nanosphere, when the laser is modulated. This study validates our model by a comparison with the results in Baffou's work.[15] Second, we will study the case of a metamaterial absorber excited by a nanosecond pulsed light. A metamaterial absorber can have high absorption in the optical regime,[22−25] which has great potential to harvest the light efficiently and generate heat in nanoscale. In our model, transient temperature distribution in the NPs and surrounding matrix can be calculated. With all input parameters from experimental conditions, our simulation discloses important temperature variation characteristics which are otherwise difficult to obtain experimentally. Our model shows that the temperature of the gold NPs rises from room temperature to 795 K in just 4 ns, when the NPs are excited by a critical light pulse fluence of 0.035 J/cm^2. Such quantitative information can be critical for designing nanostructures with functioning photothermal applications.

RESULTS AND DISCUSSION

Heat Transfer Model. Thermal analysis of the process is described by a transient heat transfer equation written as

$$C_s\rho\frac{\partial T}{\partial t}+\nabla\cdot(-k\nabla T) = Q_s \qquad (1)$$

T is the temperature of the nanostructure, both time and space dependent. C_s, ρ, and k are space-dependent specific heat capacity, density, and thermal conductivity of the material, respectively. Q_s is heat source per unit volume. The first term is the time derivative of thermal energy per unit volume. The second term is heat flux going outside the unit volume due to temperature gradient. Equation 1 is the commonly known heat transfer equation for macroscopic media. Naturally one may question its feasibility for modeling a nanoscale material system subject to a nanosecond heat source. This can be justified as follows. First, from the geometrical point of view, when a thin material film has its thickness approaching the mean free path of heat carrier, a strong boundary scattering effect drastically reduces the thermal conductivity. Such a mechanism has been well described and validated for gold film. Following the conclusion by Chen and Hui,[17] the thermal conductivity of a 60 nm-thick gold film is $k_f = 139$ W/(m·K), only 44% that of bulk gold. In view of this, we have to employ modified thermal properties for the materials used in the nanostructure according to their actual geometrical feature sizes. Second, from the temporal perspective, one has to recognize that different physical steps occurred with a clear time sequence in light−matter interaction:[4] within the first ∼100 fs, photon-electron interaction is dominant; from 100 fs to 10 ps, electron−lattice relaxation occurs; around 100 ps or longer, heat dissipation to the surrounding matrix happens. In the case of a photothermal process with a femtosecond or a picosecond pulsed light source, thermal analysis is only valid with the two-step radiation heating model,[2,3] in which electrons and lattice are defined with two distinct temperatures. Our current study however only focuses on the nanosecond heating phenomena. Therefore eq 1 is still applicable in our thermal analysis. In addition, our choice of nanosecond temporal regime, as will be shown later, corresponds to experimentally achievable situations, which facilitates cross-comparison between the theoretical and experimental results.

In the numerical analysis of heat transfer differential equations, there are two groups of boundary conditions (BCs): exterior BCs and interior BCs. Exterior BCs are conditions applied for the outermost boundaries of the geometric model. Generally, exterior BCs include Dirichlet BC, Neumann BC, and BC for the material−air interface. For Dirichlet BC, the temperature at the boundary is fixed, $T = T_{fix}$. One special case of the Neumann BC is the thermal-isolation BC and is written as $\vec{n}\cdot(-k\nabla T) = 0$, which means the normal derivative of temperature is zero. The BCs for the material−air interface is described by

$$\vec{n}\cdot(-k\nabla T) = h(T - T_r) + \varepsilon\sigma(T^4 - T_r^4) \qquad (2)$$

The term on the left represent outward conductive heat flux. The first term on the right is convective heat flux to the air environment. The second term on the right is radiation heat flux. $\vec{n}$ is the outward vector normal to the boundary surface; $h = 5$ W/(m^{2}K) is the convective heat transfer coefficient of air; ε is surface emissivity. The Stefan−Boltzmann constant is written as $\sigma = 5.67 \times 10^{-8}$ W/(m^{2}K^4). Room temperature is $T_r = 300$ K. Interior BCs are continuous conditions by default. For example, BC at the metal−water interface can

be treated as a continuous condition and described by

$$\vec{n} \cdot (-k_m \nabla T_m) = \vec{n} \cdot (-k_w \nabla T_w) \quad (3)$$

and $T_m = T_w$ at interface. k_m (k_w) and T_m (T_w) are the thermal conductivity and temperature of metal and water, respectively. When analyzing a multilayer thin film structure like metamaterial absorber,[22] one however should consider the effect of finite thermal boundary conductance (TBC). TBC is defined as

$$q = G(T_A - T_B) \quad (4)$$

where q is heat flux across the interface between materials A and B; G is TBC and $T_A - T_B$ is the temperature step of two materials at the interface. With finite TBC, the temperature of material A and material B is discontinuous at the interface. Such an interfacial effect is critical for the thermal properties of nanostructures. Previously, Käding and co-workers measured the TBC of the gold–silica interface,[18] Kato and co-workers measured the TBC of the gold–alumina interface,[19] Hopkins and co-workers studied the temperature dependence of TBC of the metal–alumina interface at high temperature and showed that TBC can be increased by 50%, when temperature rises from 300 to 500 K.[20]

Heat Generation. To calculate the heat generation within a gold NP system, the electromagnetic scattering of the nanostructure is first solved. Having the knowledge of incident field and nanostructure composition, we can solve the electromagnetic (EM) scattering problem numerically, which is done in our case with a commercial FEM solver in COMSOL Multiphysics. The lossy nature of gold, manifested by the imaginary part of its permittivity value, implies that resistive heat will be generated in the gold nanostructure.[26] The heat power volume density Q_d is written as

$$Q_d = \frac{1}{2}\varepsilon_0 \omega \, \mathrm{Im}(\varepsilon_r)|\mathbf{E}|^2 \quad (5)$$

where ε_0 is permittivity of vacuum; ω is angular frequency of the light; ε_r is the relative permittivity of gold; **E** is electric field. The optical constant of gold is referred to the experimental data measured by Johnson and Christy.[27]

Photothermal Effect of a Gold Sphere in Water. To validate our method, we conduct the EM scattering study and heat transfer study of a benchmark scenario, i.e., heating of gold sphere of 50 nm radius in water by a CW laser. Previously it was studied by Baffou with the boundary element method.[15] The gold sphere is excited by a plane wave traveling in the negative z direction with an x-polarized **E** field and an intensity of 1 mW/μm^2, shown in Figure 1a. Our EM scattering results show that the plasmon resonance of the gold sphere in water occurs at the 540 nm wavelength, with a peak absorption power of 21.45 μW, as shown in Figure 1d. With 530 nm light excitation, the normalized electric field distribution and heat power volume density Q_d around the gold sphere in water are shown in Figure 1 panels a and b, respectively. Since it is a steady-state heat transfer analysis, eq 1 is simplified such that Q_d is used as heat source Q_s and the time derivative of temperature is set to zero. The result of heat transfer analysis shows that the temperature of the gold sphere is increased by 52 K, shown in Figure 1c. These findings are similar to the results of Baffou in which a peak absorption power of 20.5 μW at wavelength 530 nm and a temperature increase of 55 K were obtained.[15] The noticeable difference is that our absorption power spectrum has a slightly broader resonance peak than Baffou's.[15]

Based on the benchmark model, we further investigate the temporal behavior of the NP system, by simulating the transient temperature variation of the nanosphere excited by an on–off modulated light source. It is well-known that the theoretical relaxation time τ_e of a gold nanosphere in water can be estimated on the basis of the heat transfer equation,[28,29]

$$\tau_e = \frac{R^2}{k/(C_s \cdot \rho)} = \frac{R^2}{\alpha} \quad (6)$$

where α is the thermal diffusivity of the material and R is the radius of the sphere. In this system, the cooling process is governed by the thermal properties of water, because the thermal conductivity of gold is two orders as high as that of water. The τ_e of a 50 nm radius sphere is 17.4 ns, where the thermal diffusivity of water α is set at 1.435×10^{-7} m^2/s. Govorov and co-worker estimated that τ_e = 6 ns for a 30 nm radius sphere.[29] The relaxation time of the gold nanosphere in water can be estimated by eq 6 only when the temperature of gold nanosphere and water are continuous at the interface. However, during the ultrafast process of femtosecond pulsed laser heating, the gold NP could reach a rather high temperature, while the temperature of water is still at 300 K. In such a case, a huge temperature gap is presented between the gold NP and water. Hu and Hartland studied the relaxation time of a gold NP excited by femtosecond laser.[5] They reported that the relaxation time is 400 ps for a gold NP with 25 nm radius, which is 10 times smaller than τ_e calculated from eq 6. In our model, we apply a nanosecond pulsed light source and restrain the gold NP system in a continuous temperature state. We simulate the temperature variation of nanospheres in water with radii of 25, 50, 75, and 100 nm, when they are heated by modulated light source. The transient temperature of a nanosphere of 50 nm radius is shown in Figure 1e, with a 110 ns rise time and a 110 ns fall time. The modulation signal has a period of 800 ns and a duty ratio of 50%. During cooling process, the temperature of a nanosphere can be fitted to a stretched

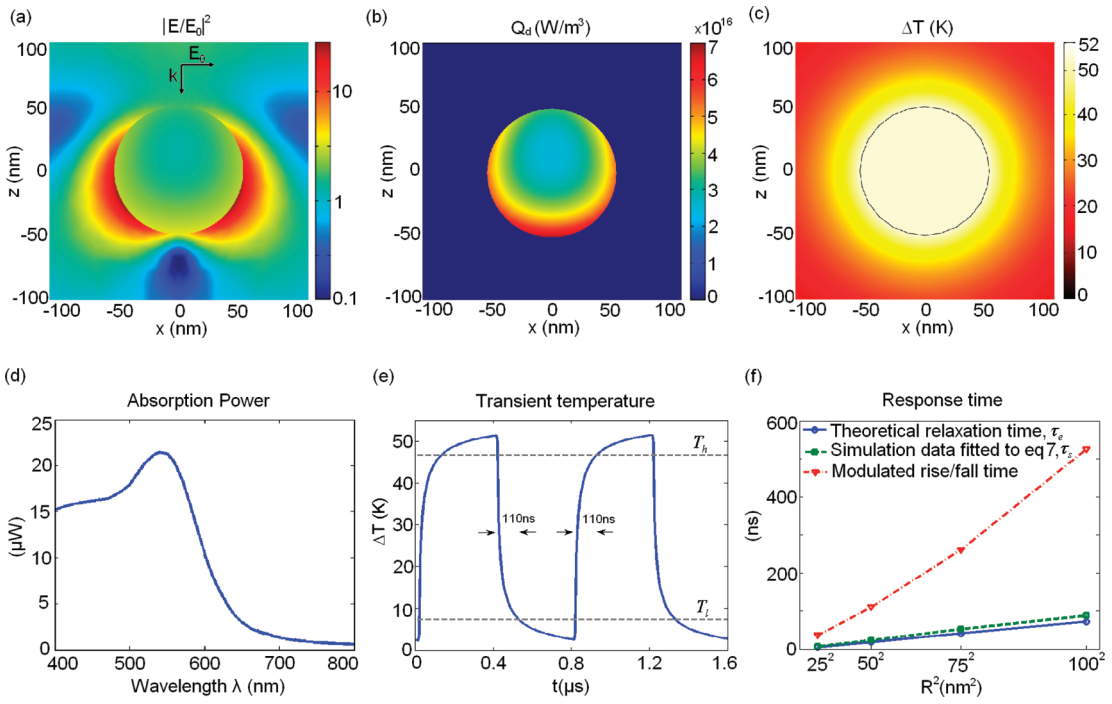

Figure 1. Photothermal effect of a gold sphere with 50 nm radius in water. (a) Electric field intensity normalized to the incident field. (b) Heat power volume density Q_d. (c) Steady-state temperature increase due to 530 nm light excitation. (d) Absorption power spectrum of gold sphere in water, with incident light intensity at 1 mW/μm^2. (e) Transient temperature of R = 50 nm gold nanosphere in water excited by on−off modulated light. (f) Comparison of theoretical relaxation time τ_e, relaxation time fit to simulation result τ_s, and modulated rise/fall time of gold nanosphere as a function of R^2.

exponential function purposed by Hu and Hartland[5] as

$$F(t) = A \exp\left(-\left(\frac{t - t_{off}}{\tau_s}\right)^{\beta}\right) \quad (7)$$

where t_{off} is the moment when the heat source is turned off; A is the temperature of the nanosphere at $t = t_{off}$; the relaxation time τ_s can be derived by fitting the simulated temperature data to eq 7; the stretching parameter β equals 0.4 for a 50 nm-radius nanosphere. The simulated relaxation time τ_s derived by fitting simulation data to eq 7 is compared with τ_e as a function of R^2, shown in Figure 1f. It indicates that τ_s is a linear function of R^2 and 27% larger than τ_e. We also extract the rise/fall time from the modulated temperature of nanospheres with various radii. We define two threshold levels T_h and T_l of the modulated temperature, as shown in Figure 1e. T_h sits at the 90% of temperature step and T_l sits at the 10% of temperature step. The rise/fall time is defined as the time interval for temperature to change from T_l to T_h or *vice versa*. In Figure 1f, the rise/fall time is also compared with τ_e and τ_s as a function of R^2. The rise/fall time is approximately 5 times as long as τ_s, which is mainly due to the fact that the rise/fall time is corresponding to a larger change from 90% to 10%, while relaxation time τ_s corresponds to a smaller change from 100% to $1/e$ = 36.8%. In this study, the permittivity of water is considered to be 1.777, and the material thermal properties are listed in Table 1.

TABLE 1. Material Thermal Properties Used in the Heat Transfer Model

	specific heat capacity, C_s (J/(kg·K))	density, ρ (kg/m^3)	thermal conductivity, k (W/(m·K))
gold	129	19300	317 (bulk), 139 (thickness = 60 nm), 110 (thickness = 40 nm)
water	4180	1000	0.6
alumina	880	3980	6
silica	741	2200	1
air	1	353[K]/T, 1.18 (T = 300 K), 0.44 (T = 800 K)	0.03

Photothermal Effect of Metamaterial Absorber. We apply our method to a more complicated study case, that is, a photothermal effect in a metamaterial absorber excited by a nanosecond pulsed light source. Figure 2a shows one unit cell of the three-layer metamaterial absorber used in our experiment. A single unit can be treated as an optical resonator. The units are arranged to form a two-dimensional square lattice with lattice constant a = 310 nm in both x and y direction. The structure has three key layers: a 40 nm-thick gold particle on the top; a 10 nm-thick alumina spacer in the middle; and a 60 nm-thick gold film in the substrate. The upper half space is air and the sample is on a 150 μm-thick BK7 silica glass. The gold particle has a size of 230 × 170 nm^2 in xy dimension.

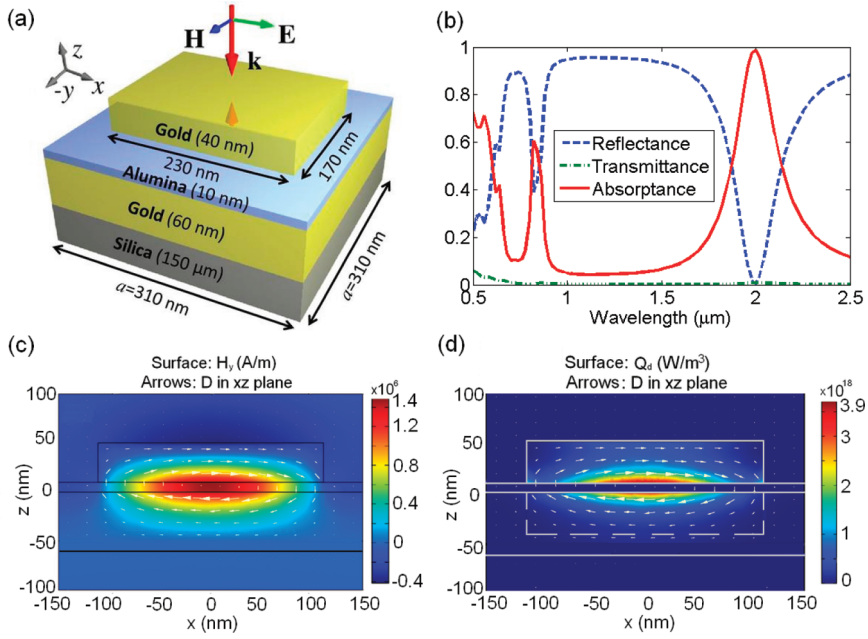

Figure 2. (a) Geometric structure and material composition of three-layer metamaterial absorber. The orientation of electric field E and wave vector k of the incident light is also shown. (b) Simulated spectra of reflectance, transmittance and absorptance of metamaterial absorber. (c) Magnetic field H is shown as color image. Electric displacement D is shown as arrows, in the absorber unit cell with incidence of *x*-polarized light at 2.0 μm wavelength. (d) Heat power volume density Q_d of the absorber unit cell with incidence of *x*-polarized light at 2.0 μm wavelength. At plasmon resonance, Q_d is strongly localized within gold NP (upper gray solid line box) and its mirror symmetric counterpart (lower gray dash line box).

The absorber sample is normally excited by a supercontinuum light source with a wavelength range from 500 to 2400 nm. The light source has a repetition rate f_r = 25 kHz and pulse duration of 2.6 ns. The light is *x*-polarized with the **E** field only in the *x* direction, as shown in Figure 2a. The obtained reflectance, transmittance, and absorptance spectra, as well as the EM field distribution over the sample are shown in Figure 2b. In Figure 2b, the first resonance peak is clearly seen at 2.0 μm with near unity absorptance. It indicates that the 3-layer absorber is a highly efficient device for light energy harvest. At a plasmon resonance of 2.0 μm wavelength, the magnetic field **H** is localized within the gap between the gold NP and the gold film, while the electric displacement vector **D** forms a loop around the gap, as shown in Figure 2c. It indicates that the EM energy is mainly concentrated within and around the gap region with dimensions less than $^1/_8$ of the wavelength.

The heat power volume density Q_d at a resonance of 2.0 μm wavelength is shown in Figure 2d. We categorize the heat source distribution into three regions, the top layer gold NP, the mirror-symmetric counterpart of NP within the gold film (region with dash line box shown in Figure 2d) and the rest of gold film. The resistive heat is dependent on the wavelength and the polarization of the incidence light. In Table 2, the heat source distribution of the absorber unit cell is shown, with normal incident *x*-polarized light at wavelength of 2.5 μm (off resonance), 2.0 μm (first resonance), and 0.82 μm (second resonance). It is found that the dominant portion of heat source is in the top layer gold NP at the plasmon resonance. For the off-resonance case, the heat source distribution is more evenly distributed within the three regions. Moreover, the optical absorptances at the plasmon resonance of 2.0 and 0.82 μm are 0.98 and 0.60, respectively, at least 5 times higher than the absorptance at the off-resonance of 2.5 μm, as shown in Figure 2b. It indicates that the plasmon resonance of a gold NP system greatly enhances the heat power generation and localization during the photothermal process.

TABLE 2. Heat Source Distribution of an Absorber Unit Cell with Incidence of *x*-Polarized Light

	off resonance, wavelength = 2.5 μm	first resonance, wavelength = 2.0 μm	second resonance, wavelength = 0.82 μm
the top layer gold NP	39.2%	64.8%	62.1%
the mirror symmetric counterpart of NP in gold film	37.7%	27.6%	31.1%
the rest of gold film	23.1%	7.6%	6.7%

The intensity of the incident light beam on the sample has a Gaussian profile with a 20 μm measured spot diameter. The light fluence shining on the sample from a single pulse is written as

$$F_l(r) = \frac{2P_0}{\pi w^2 f_r} \exp\left(-\frac{2r^2}{w^2}\right) \quad (8)$$

In eq 8, P_0 = 2.3 mW is the total optical power of the incident light irradiating on the sample.

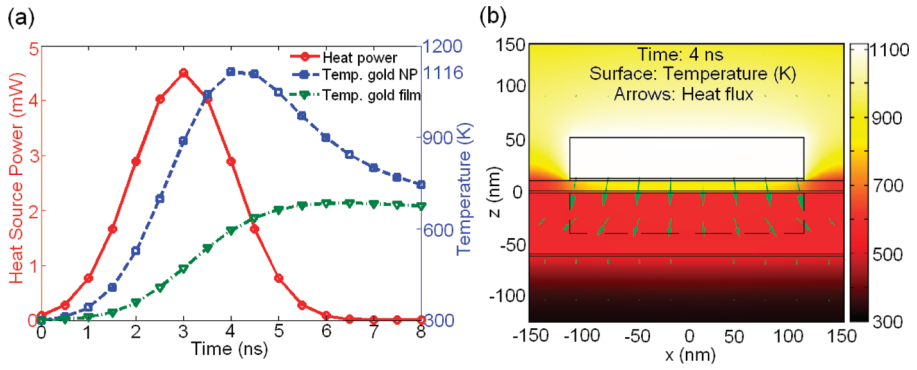

Figure 3. (a) Heat power irradiating on an absorber unit cell located at the beam center and temperatures of gold NP and gold film in such a unit cell during one pulse. (b) In the cross section view of the one absorber unit cell, the color image indicates temperature distribution at 4.0 ns. The arrows indicate the heat flux at the same time.

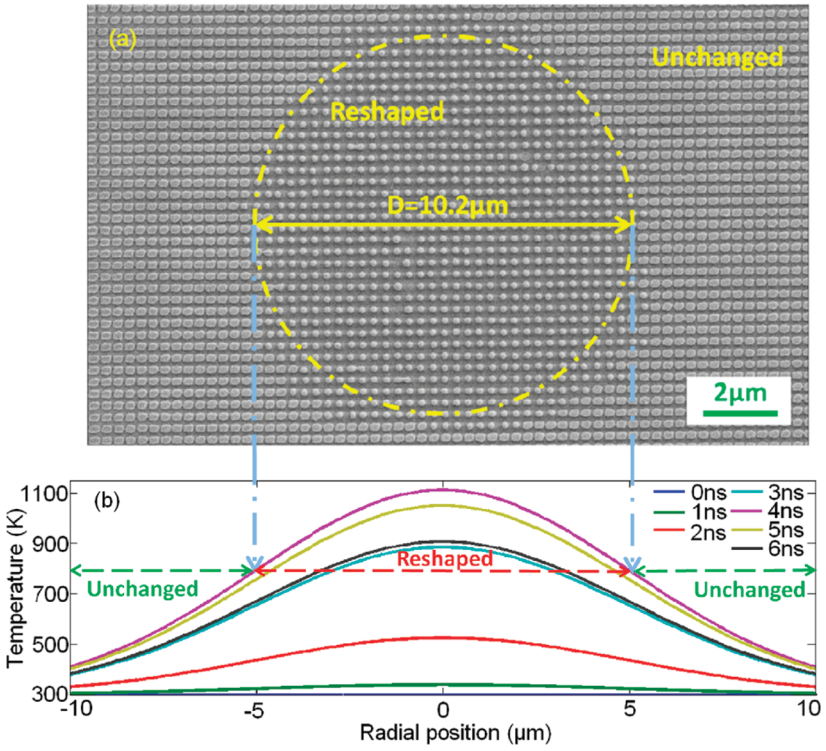

Figure 4. (a) Top view scanning electron microscope image of absorber sample after light exposure of 0.2 s. At circle center, light fluence of a single pulse is 0.059 J/cm^2; while at the circle boundary, light fluence of a single pulse is 0.035 J/cm^2. (b) Calculated radial distribution of temperature of gold NPs during one light pulse from 0 to 6 ns.

f_r = 25 kHz is the pulse repetition rate; r is the distance from the beam center; w = 10 μm is the Gaussian beam waist. At the beam center, the light fluence is 0.059 J/cm^2. The optical energy over one unit cell is

$$E_{op}(r) = a^2 F_l(r) \quad (9)$$

where a = 310 nm is the lattice constant of the NP array. At the beam center, $E_{op}(0)$ = 56.3 pJ. The thermal energy absorbed by one unit cell is

$$E_{th}(r) = R_a E_{op}(r) \quad (10)$$

where R_a the absorption coefficient of the metamaterial absorber is 0.213, derived from the overlap integral between the light source power density spectrum and the metamaterial absorptance spectrum, shown in Figure 2b, in the range from 0.5 to 2.5 μm. For the unit cell at beam center, thermal energy is written as

$$E_{th}(0) = 0.213 \times 56.3 \text{ pJ} = 12.0 \text{ pJ} \quad (11)$$

The nanosecond heat source is finally described by a Gaussian pulse function,

$$Q_s(r,t) = \frac{E_{th}(r)}{\Delta V}\frac{1}{\sqrt{\pi}\tau}\exp\left(-\frac{(t-t_0)^2}{\tau^2}\right) \quad (12)$$

where ΔV is the volume of heat source, τ = 1.5 ns is the time constant of the light pulse, t_0 = 3 ns is the time delay of the pulse peak.

The transient heat transfer problem is solved by the FEM with COMSOL. As an example, the absorber unit cell located at the center of Gaussian light beam is modeled and analyzed first. At Gaussian beam center, the temperatures of the gold NP T_p and the gold film T_f during the heat pulse are shown in Figure 3a. T_p reaches maximum 1116 K at 4.0 ns. Due to heat dissipation to the surrounding, T_p drops to 330 K after 1 μs; 40 μs later, T_p drops to 300.5 K, just before the next pulse comes. The temperature distribution of one absorber unit cell at 4.0 ns is shown in Figure 3b. The temperature within the gold NP is uniform, due to the high thermal conductivity of gold and its small particle size. The dominant temperature gradient is along $-z$ direction, indicating that the BK7 glass substrate is an effective heat sink in our model. A rather large temperature difference of 522 K between the top gold NP and the bottom gold film is clearly shown during the transition. If the finite TBC effect at the gold–alumina and gold–silica interfaces is not considered in the heat transfer model, the temperature of the gold NP reaches its maximum of 751 K at 4.5 ns, and the temperature difference between gold NP and gold film is merely 40 K at that moment. It implies that a finite TBC can drastically elevate temperature inhomogeneity in a multilayer nanostructure.

We conducted an experiment of photothermal reshaping of gold NPs in metamaterial absorber with a nanosecond pulsed light. The NPs reshaping phenomena can be elaborated with our numerical heat transfer analysis. In Figure 4a, the scanning electron microscope (SEM) picture of a sample after it is irradiated by the mentioned light source is shown. Because of high optical absorbance and localized heat generation of the nanoscale absorber, the concentrated heat power is able to cause the morphology change of the gold NPs in the absorber sample. In Figure 4a, a clear circular boundary of 10.2 μm in diameter divides the sample into two zones. Inside the circle, the top layer rectangular shape gold NPs are transformed to spherical dome shape with 160 nm diameter; while outside the circle, the shapes of the gold NPs are unchanged. According to our heat transfer analysis, the maximum temperature of gold NP at the circle center is 1116 K, corresponding to a fluence of 0.059 J/cm^2 for a single pulse. According to the Gaussian beam intensity distribution, the maximum temperature of gold NPs located on the critical circle boundary is 795 K, corresponding to F_l (5.1 μm) = 0.035 J/cm^2. With heat transfer analysis, the calculated radial distribution of gold NPs temperature vividly presents the photothermal process in a quantitative manner, as shown in Figure 4b. The center region with a temperature above 795 K corresponds to the reshaped zone in Figure 4a; while the region with lower temperature corresponds to an unchanged zone. The experiment indicates that with photothermal treatment, gold NPs can undergo reshaping at a critical temperature of 795 K, much lower than the melting point of bulk gold 1337 K. The morphology change of metal NPs below the bulk melting point can be explained by theory of surface melting.[6,7] Previous study by Magnusson and coworkers[30] has shown gold NPs reshaping to a near spherical shape of 40 nm in diameter, using gas phase thermal annealing at 500 K. In our case, the photothermal reshaped NP is much larger, 160 nm in diameter. It is reasonable that our critical temperature is higher than 500 K, because the binding energy of metal crystal in NP increases with larger particle size.

CONCLUSIONS

A heat transfer model is built to resolve the transient temperature variation in metal nanostructure during a photothermal process. We study the photothermal process of two plasmonic nanostructures. First, the CW-laser heating of a gold nanosphere in water is investigated. The thermal relaxation time of a nanosphere in water is numerically derived and compared to the well-known analytical relaxation time $\tau_e = R^2/\alpha$. The photothermally induced rise/fall time of a nanosphere in temperature is found to be 5 times τ_s. Second, the heating and reshaping of the gold NPs in a metamaterial structure induced by a nanosecond-pulsed light source is investigated. Our model predicts that the reshaping of gold NPs takes place at only 795 K, induced by critical pulse fluence of 0.035 J/cm^2. The thermal response time in both cases is all at the nanosecond scale. The model presented can be valuable for quantitatively analyzing photothermal effects in various plasmonic systems, which can have promising applications in biology, optical storage, and thermophotovoltaic technology.

MATERIALS AND METHODS

Solving Electromagnetic Scattering of Metamaterial Absorber with FEM Method. Metamaterial absorber is composed of 2D square array of unit cells, shown as in Figure 2a. The incident light is normal to the *xy* plane with **E** field polarized in *x* direction. To account for the periodic nature of the metamaterial absorber, the model boundary at $x = \pm a/2$ and $y = \pm a/2$ is set to condition of perfect electric conductor and perfect magnetic conductor, respectively. The refractive indices of air, silica, and alumina are 1, 1.45, and 1.73, respectively. The optical constant of gold is taken from the data of Johnson and Christy.[27] The details about electromagnetic scattering of metamaterial absorber can be referred to the work by Hao *et al.*[14]

Solving Heat Transfer Model of Metamaterial Absorber with FEM Method. To solve the heat transfer model, the following four pieces of information are essential: geometric structure, thermal material properties, boundary condition, and heat source. The geometric structure of a unit cell is shown in Figure 2a and is mentioned when solving the EM scattering problem. Material thermal properties used in our heat transfer model are listed in

Table 1, where the density of air at atmospheric pressure can be calculated using the ideal gas law. For a unit cell of absorber as shown in Figure 2a, at the upper boundary plane in the z direction, the boundary condition is described by eq 2, which includes convective and irradiative heat exchange. At the lower boundary plane in the z direction, the temperature of the silica substrate is set to room temperature at 300 K. At the boundary planes of $x = \pm a/2$ and $y = \pm a/2$, the heat flux in the horizontal direction is set to zero. Setting the horizontal heat flux to zero at the x and y boundaries is equivalent to setting periodic conditions at these boundaries, therefore the unit cell is no longer treated as a stand alone object, but as an element of a 2D square array with a lattice constant a. Noticeably, at the interior boundaries of the absorber unit cell, the finite TBC of the gold−alumina interfaces and gold−silica interface could lead to significant temperature discontinuity at these interfaces, when vertical heat flux is present in the unit cell. To incorporate the TBC effect in our numerical calculation, thin layers of fictitious material with specific thickness and thermal conductivity are inserted into the model at these interfaces. The thin layer of fictitious material can mimic the temperature discontinuity caused by TBC at the interface of material A and material B, if the parameters follow the rule:

$$q = G(T_A - T_B) = k_e \frac{(T_A - T_B)}{d} \quad (13)$$

where k_e and d are the thermal conductivity and thickness of the fictitious film; the second term is a heat flux at the A−B interface with temperature discontinuity; the third term is heat flux through a fictitious film with a temperature gradient. In such a way, the temperature discontinuity is avoided, while the consistency of temperature difference and heat flux is kept. In our model, the TBC of the gold−alumina interface is 135×10^6 W/(m^2·k) and the TBC of the gold−silica interface is 187×10^6 W/(m^2·k). With d = 2 nm, the k_e of the fictitious film is 0.270 W/(m·k) and 0.375 W/(m·k) for the gold−alumina interface and gold−silica interface, respectively. Defined in eq 12, Q_s represents the total heat power of one arbitrary absorber unit cell. However, Q_d represents volume density of heat power within such unit cell, as shown in Figure 2d. In the heat transfer model, Q_d is normalized, so that the volume integral of Q_d over the unit cell equals Q_s. In such a way, our model incorporates both the localized distribution of the heat source within the nanostructure derived from the EM scattering problem and the actual heat source power derived from experiment configuration.

Conflict of Interest: The authors declare no competing financial interest.

Acknowledgment. We thank Jing Wang for the fabrication of the sample and Jiaming Hao for designing of the metamaterial absorber. This work is supported by the Swedish Foundation for Strategic Research (SSF) and the Swedish Research Council (VR).

REFERENCES AND NOTES

1. Kaganov, M. I.; Lifshitz, I. M.; Tanatarov, L. V. Relaxation between Electrons and Crystalline Lattices. *Sov. Phys. JETP.* **1957**, *4*, 173–178.
2. Anisimov, S. I.; Kapeliovich, B. L.; Perel'Man, T. L. Electron Emission from Metal Surfaces Exposed to Ultra-Short Laser Pulses. *Sov. Phys. JETP.* **1974**, *39*, 375–377.
3. Qiu, T.; Tien, C. Short-Pulse Laser Heating on Metals. *Int. J. Heat Mass Transfer* **1992**, *35*, 719–726.
4. Link, S.; Burda, C.; Nikoobakht, B.; El-Sayed, M. A. Laser-Induced Shape Changes of Colloidal Gold Nanorods Using Femtosecond and Nanosecond Laser Pulses. *J. Phys. Chem. B* **2000**, *104*, 6152–6163.
5. Hu, M.; Hartland, G. V. Heat Dissipation for Au Particles in Aqueous Solution: Relaxation Time *versus* Size. *J. Phys. Chem. B* **2002**, *106*, 7029–7033.
6. Plech, A.; Kotaidis, V.; Grésillon, S.; Dahmen, C.; von Plessen, G. Laser-Induced Heating and Melting of Gold Nanoparticles Studied by Time-Resolved X-ray Scattering. *Phys. Rev. B* **2004**, *70*, 195423.
7. Plech, A.; Cerna, R.; Kotaidis, V.; Hudert, F.; Bartels, A.; Dekorsy, T. A Surface Phase Transition of Supported Gold Nanoparticles. *Nano Lett.* **2007**, *7*, 1026–1031.
8. Govorov, A. O.; Richardson, H. H. Generating Heat with Metal Nanoparticles. *Nano Today* **2007**, *2*, 30–38.
9. Baffou, G.; Girard, C.; Quidant, R. Mapping Heat Origin in Plasmonic Structures. *Phys. Rev. Lett.* **2010**, *104*, 136805.
10. Kuznetsov, A. I.; Evlyukhin, A. B.; Goncalves, M. R.; Reinhardt, C.; Koroleva, A.; Arnedillo, M. L.; Kiyan, R.; Marti, O.; Chichkov, B. N. Laser Fabrication of Large-Scale Nanoparticle Arrays for Sensing Applications. *ACS Nano* **2011**, *5*, 4843–4849.
11. Sun, F.; Cai, W.; Li, Y.; Duan, G.; Nichols, W.; Liang, C.; Koshizaki, N.; Fang, Q.; Boyd, I. Laser Morphological Manipulation of Gold Nanoparticles Periodically Arranged on Solid Supports. *Appl. Phys. B: Lasers Opt.* **2005**, *81*, 765–768.
12. Huang, X.; El-Sayed, I. H.; Qian, W.; El-Sayed, M. A. Cancer Cell Imaging and Photothermal Therapy in the Near-Infrared Region by Using Gold Nanorods. *J. Am. Chem. Soc.* **2006**, *128*, 2115–2120.
13. Yavuz, M. S.; Cheng, Y.; Chen, J.; Cobley, C. M.; Zhang, Q.; Rycenga, M.; Xie, J.; Kim, C.; Song, K. H.; Schwartz, A. G.; *et al.* Gold Nanocages Covered by Smart Polymers for Controlled Release with Near-Infrared Light. *Nat. Mater.* **2009**, *8*, 935–939.
14. Zijlstra, P.; Chon, J. W. M.; Gu, M. Five-Dimensional Optical Recording Mediated by Surface Plasmons in Gold Nanorods. *Nature* **2009**, *459*, 410–413.
15. Baffou, G.; Quidant, R.; Garcia de Abajo, F. J. Nanoscale Control of Optical Heating in Complex Plasmonic Systems. *ACS Nano* **2010**, *4*, 709–716.
16. Baffou, G.; Rigneault, H. Femtosecond-Pulsed Optical Heating of Gold Nanoparticles. *Phys. Rev. B* **2011**, *84*, 035415.
17. Chen, G.; Hui, P. Thermal Conductivities of Evaporated Gold Films on Silicon and Glass. *Appl. Phys. Lett.* **1999**, *74*, 2942–2944.
18. Käding, O. W.; Skurk, H.; Goodson, K. E. Thermal Conduction in Metallized Silicon-Dioxide Layers on Silicon. *Appl. Phys. Lett.* **1994**, *65*, 1629–1631.
19. Kato, R.; Xu, Y.; Goto, M. Development of a Frequency-Domain Method Using Completely Optical Techniques for Measuring the Interfacial Thermal Resistance between the Metal Film and the Substrate. *Jpn. J. Appl. Phys.* **2011**, *50*, 106602.
20. Hopkins, P.; Salaway, R.; Stevens, R.; Norris, P. Temperature-Dependent Thermal Boundary Conductance at Al/Al_2O_3 and Pt/Al_2O_3 Interfaces. *Int. J. Thermophys.* **2007**, *28*, 947–957.
21. Buffat, P.; Borel, J.-P. Size Effect on the Melting Temperature of Gold Particles. *Phys. Rev. A* **1976**, *13*, 2287–2298.
22. Hao, J.; Wang, J.; Liu, X.; Padilla, W. J.; Zhou, L.; Qiu, M. High Performance Optical Absorber Based on a Plasmonic Metamaterial. *Appl. Phys. Lett.* **2010**, *96*, 251104.
23. Wang, J.; Chen, Y.; Hao, J.; Yan, M.; Qiu, M. Shape-Dependent Absorption Characteristics of Three-Layered Metamaterial Absorbers at Near-Infrared. *J. Appl. Phys.* **2011**, *109*, 074510.
24. Hao, J.; Zhou, L.; Qiu, M. Nearly Total Absorption of Light and Heat Generation by Plasmonic Metamaterials. *Phys. Rev. B* **2011**, *83*, 165107.
25. Wang, J.; Chen, Y.; Chen, X.; Hao, J.; Yan, M.; Qiu, M. Photothermal Reshaping of Gold Nanoparticles in a Plasmonic Absorber. *Opt. Express* **2011**, *19*, 14726–14734.
26. Loudon, R. The Propagation of Electromagnetic Energy through an Absorbing Dielectric. *J. Phys. A: Gen. Phys.* **1970**, *3*, 233–245.
27. Johnson, P. B.; Christy, R. W. Optical Constants of the Noble Metals. *Phys. Rev. B* **1972**, *6*, 4370–4379.
28. Fred, C. Heat Transfer from a Sphere to an Infinite Medium. *Int. J. Heat Mass Transfer* **1977**, *20*, 991–993.
29. Govorov, A.; Zhang, W.; Skeini, T.; Richardson, H.; Lee, J.; Kotov, N. Gold Nanoparticle Ensembles as Heaters and Actuators: Melting and Collective Plasmon Resonances. *Nanoscale Res. Lett.* **2006**, *1*, 84–90.
30. Magnusson, M. H.; Deppert, K.; Malm, J.-O.; Bovin, J.-O.; Samuelson, L. Gold Nanoparticles: Production, Reshaping and Thermal Charging. *J. Nanopart. Res.* **1999**, *1*, 243–251.